J|A|C|S
ARTICLES
Published on Web 08/02/2003

Melem (2,5,8-Triamino-tri-*s*-triazine), an Important Intermediate during Condensation of Melamine Rings to Graphitic Carbon Nitride: Synthesis, Structure Determination by X-ray Powder Diffractometry, Solid-State NMR, and Theoretical Studies

Barbara Jürgens,[†] Elisabeth Irran,[‡] Jürgen Senker,[†] Peter Kroll,[§] Helen Müller,[†] and Wolfgang Schnick*[,†]

Contribution from the Ludwig-Maximilians-Universität München, Department Chemie, Butenandtstrasse 5-13 (D), D-81377 München, Germany, Institut für Chemie − Anorganische Festkörperchemie, Sekr. C2, TU Berlin, Strasse des 17. Juni 135, D-10623 Berlin, Germany, and Institut für Anorganische Chemie, RWTH Aachen, Professor-Pirlet-Strasse 1, D-52056 Aachen, Germany

Received April 24, 2003; E-mail: wolfgang.schnick@uni-muenchen.de

Abstract: Single-phase melem (2,5,8-triamino-tri-*s*-triazine) $C_6N_7(NH_2)_3$ was obtained as a crystalline powder by thermal treatment of different less condensed C−N−H compounds (e.g., melamine $C_3N_3(NH_2)_3$, dicyandiamide $H_4C_2N_4$, ammonium dicyanamide $NH_4[N(CN)_2]$, or cyanamide H_2CN_2, respectively) at temperatures up to 450 °C in sealed glass ampules. The crystal structure was determined ab initio by X-ray powder diffractometry (Cu Kα_1: $P2_1/c$ (No. 14), a = 739.92(1) pm, b = 865.28(3) pm, c = 1338.16(4) pm, β = 99.912(2)°, and Z = 4). In the solid, melem consists of nearly planar $C_6N_7(NH_2)_3$ molecules which are arranged into parallel layers with an interplanar distance of 327 pm. Detailed ^{13}C and ^{15}N MAS NMR investigations were performed. The presence of the triamino form instead of other possible tautomers was confirmed by a CPPI (cross-polarization combined with polarization inversion) experiment. Furthermore, the compound was characterized using mass spectrometry, vibrational (IR, Raman), and photoluminescence spectroscopy. The structural and vibrational properties of molecular melem were theoretically studied on both the B3LYP and the MP2 level. A structural optimization in the extended state was performed employing density functional methods utilizing LDA and GGA. A good agreement was found between the observed and calculated structural parameters and also for the vibrational frequencies of melem. According to temperature-dependent X-ray powder diffractometry investigations above 560 °C, melem transforms into a graphite-like C−N material.

Melamine (2,4,6-triamino-*s*-triazine), $C_3N_3(NH_2)_3$ **1a**, represents an important starting material for several industrial applications, for example, the syntheses of melamine-formaldehyde resins or of fireproof materials.[1,2] Furthermore, it is used for the architecture of supramolecular structures, for example, assemblies built up by cyanuric acid $C_3N_3(OH)_3$ **1b** or melamine derivatives.[3−5] In the past few years, another interest arose in melamine as well as in other compounds, $C_3N_3X_3$ **1**, containing *s*-triazine (cyanuric) rings C_3N_3, for example, cyanuric chloride $C_3N_3Cl_3$ **1c**[6−10] or cyanuric azide $C_3N_3(N_3)_3$ **1d**.[11] These are considered to be suitable molecular precursor compounds for the synthesis of graphitic forms of carbon nitride (g-C_3N_4).[6,12−14] In most of the postulated structures of g-C_3N_4, *s*-triazine ring systems are linked through trigonal N atoms forming extended 2D sheets **2** (Scheme 1).

Recently, another possible building block for g-C_3N_4 was taken into account (Scheme 2): tri-*s*-triazine rings C_6N_7 which are cross-linked by trigonal N atoms **3**.[15−17] The possible condensation of three *s*-triazine rings and the existence of a "cyameluric nucleus" C_6N_7 **4** was first postulated by Pauling

[†] Ludwig-Maximilians-Universität München.
[‡] TU Berlin.
[§] RWTH Aachen.

(1) Allcock, H. R.; Lampe, F. W. *Contemporary Polymer Chemistry*; Prentice Hall: New Jersey, 1990.
(2) Kuryla, W. C.; Papa, A. J. *Flame Retardancy of Polymeric Materials*; Dekker: New York, 1973−1979; Vols. 1−5.
(3) Lindoy, L. F.; Atkinson, I. M. *Self-assembly in Supramolecular Systems*; Monographs in Supramolecular Chemistry, issue 7; Cambridge: New York, 2000.
(4) Steed, J. W.; Atwood, J. L. *Supramolecular Chemistry*; John Wiley & Sons, Ltd.: Chichester, New York, Weinheim, Brisbane, Singapore, Toronto, 2000.
(5) Kimizuka, N.; Kawasaki, T.; Hirata, K.; Kunitake, T. *J. Am. Chem. Soc.* **1995**, *117*, 6360.
(6) Alves, I.; Demazeau, G.; Tanguy, B.; Weill, F. *Solid State Commun.* **1999**, *109*, 697.
(7) Zhang, Z.; Leinenweber, K.; Bauer, M.; Garvie, L. A. J., McMillan, P. F.; Wolf, G. H. *J. Am. Chem. Soc.* **2001**, *123*, 7788.
(8) Wolf, G. H.; Bauer, M.; Leinenweber, K.; Garvie, L. A. J.; Zhang, Z. *NATO Sci. Ser., II: Mathematics, Physics and Chemistry* **2001**, *48 (Frontiers of High-Pressure Research II: Application of High Pressure to Low-Dimensional Novel Electronic Materials)*, 29.
(9) Kawaguchi, M.; Nozaki, K. *Chem. Mater.* **1995**, *7*, 257.
(10) Khabashesku, V. N.; Zimmermann, J. L.; Margrave, J. L. *Chem. Mater.* **2000**, *12*, 3264.
(11) Gillan, E. G. *Chem. Mater.* **2000**, *12*, 3906.
(12) Liu, A. Y.; Cohen, M. L. *Science* **1989**, *245*, 841.
(13) Teter, D. M.; Hemley, R. J. *Science* **1996**, *271*, 53.
(14) Mattesini, M.; Matar, S. F.; Etourneau, J. *J. Mater. Chem.* **2000**, *10*, 709.
(15) Komatsu, T. *J. Mater. Chem.* **2001**, *11*, 802.
(16) Komatsu, T.; Nakamura, T. *J. Mater. Chem.* **2001**, *11*, 474.
(17) Kroke, E.; Schwarz, M.; Horath-Bordon, E.; Kroll, P.; Noll, B.; Norman, A. D. *New J. Chem.* **2002**, *26*, 508.

10.1021/ja0357689 CCC: $25.00

Scheme 1. *s*-Triazines

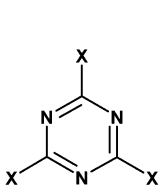

1

1a: **X = NH_2**
1b: **X = OH**
1c: **X = Cl**
1d: **X = N_3**
1e: **X = NCNH**

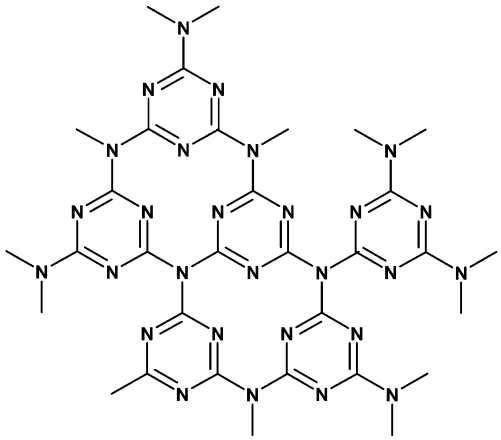

2

Scheme 2. Tri-*s*-triazines

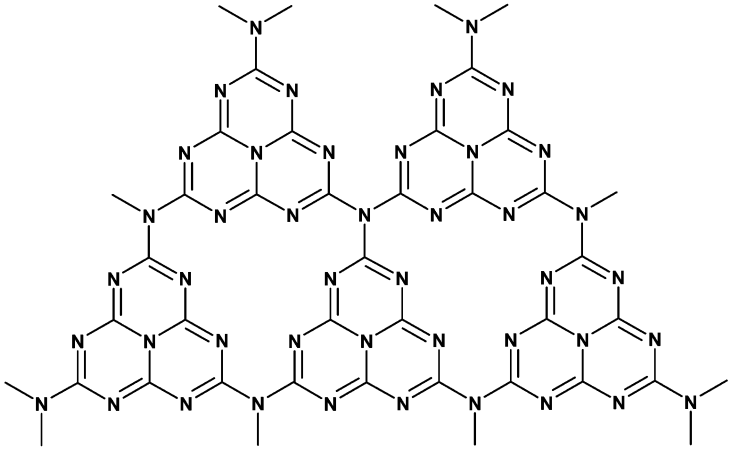

3

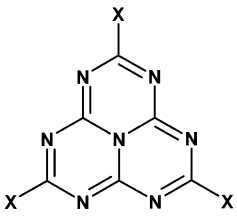

4

4a: **X = OH**
4b: **X = NCNH**
4c: **X = H**
4d: **X = Cl**
4e: **X = NH_2**

and Sturdivant.[18] On the basis of this complex ring system, further substitutional derivatives were predicted in analogy to compounds containing the cyanuric ring, for example, cyameluric acid $C_6N_7(OH)_3$ **4a** which is related to cyanuric acid $C_3N_3(OH)_3$ or hydromelonic acid $C_6N_7(NCNH)_3$ **4b** which represents the analogue to postulated tricyanomelamine $C_3N_3(NCNH)_3$ **1e**.[19] Many attempts were performed to synthesize and characterize cyameluric derivatives; however, the existence of the C_6N_7 ring system has been proven lately with the crystal structure of tri-*s*-triazine $C_6N_7H_3$ **4c**.[20−21] Very recently, Kroke et al. described the first functionalized derivative, trichloro-tri-*s*-triazine $C_6N_7Cl_3$ **4d**.[17]

In analogy to **2** where 2,4,6-triamino-*s*-triazine represents the repeating unit, 2,5,8-triamino-tri-*s*-triazine **4e** can be considered as the repeating unit of **3**. Synonyms for 2,5,8-triamino-tri-*s*-triazine are 2,5,8-triamino-1,3,4,6,7,9,9*b*-heptaazaphenalene or 2,5,8-triamino-1,3,4,6,7,9-hexaazacycl[3.3.3]azine and 2,5,8-triamino-*s*-heptazine. The trivial name melem for compound **4e** dates back to Liebig who performed different experiments with carbon nitrides:[22] While heating potassium thiocyanate with ammonium chloride, he obtained **1a** which he named melamine. Later, the formation of melamine by different other experiments was observed, for example, by heating cyanamide H_2CN_2 **5**, ammonium dicyanamide $NH_4[N(CN)_2]$ **6**, or dicyandiamide $H_4C_2N_4$ **7** (Scheme 3).[23−25]

The pyrolysis of melamine as well as its behavior under pressure were investigated, and condensation processes (Scheme 4) leading to so-called melam **8**, melem **4e**, and melon **9** were postulated.[26−30] For melamine, structural data have been reported. Neither the existence of melam nor the existence of melem and melon could be confirmed by crystal structure determinations as yet.[31,32]

(18) Pauling, L.; Sturdivant, J. H. *Proc. Natl. Acad. Sci. U.S.A.* **1937**, *23*, 615.
(19) Redemann, C. E.; Lucas, H. J. *J. Am. Chem. Soc.* **1940**, *62*, 842.
(20) Hosmane, R. S.; Rossman, M. A.; Leonard, N. J. *J. Am. Chem. Soc.* **1982**, *104*, 5497.
(21) Shahbaz, M.; Urano, S.; LeBreton, P. R.; Rossman, M. A.; Hosmane, R. S.; Leonard, N. J. *J. Am. Chem. Soc.* **1984**, *106*, 2805.
(22) Liebig, J. *Ann. Chem.* **1834**, *10*, 1.
(23) Bieling, H.; Radüchel, M.; Wenzel, G.; Beyer, H. *J. Prakt. Chem.* **1965**, *28*, 325.
(24) Jürgens, B.; Höppe, H. A.; Irran, E.; Schnick, W. *Inorg. Chem.* **2002**, *41*, 4849.
(25) Franklin, E. C. *J. Am. Chem. Soc.* **1922**, *44*, 486.
(26) May, H. *J. Appl. Chem.* **1959**, 340.
(27) van der Plaats, G.; Soons, H.; Snellings, R. *Proc. Eur. Symp. Therm. Anal.* **1981**, *2*, 215.
(28) Purdy, A. P.; Callahan, J. H. *Main Group Chem.* **1998**, *2*, 207.
(29) Ma, H. A.; Jia, X.; Cui, Q. L.; Pan, Y. W.; Zhu, P. W.; Liu, B. B.; Liu, H. J.; Wang, X. C.; Liu, J.; Zou, G. T. *Chem. Phys. Lett.* **2003**, *368*, 668.
(30) Costa, L.; Camino, G. *J. Calorim., Anal. Therm. Thermodyn. Chim.* **1986**, *17*, 213.
(31) Larson, A. C.; Cromer, D. T. *J. Chem. Phys.* **1974**, *60*, 185.

Scheme 3. Formation of Melamine **1a**

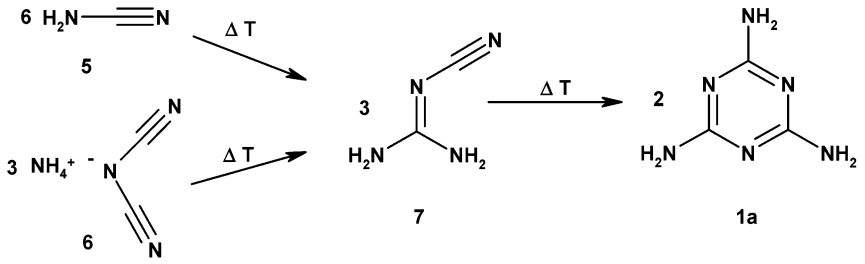

Scheme 4. Postulated Condensation of Melamine **1a**

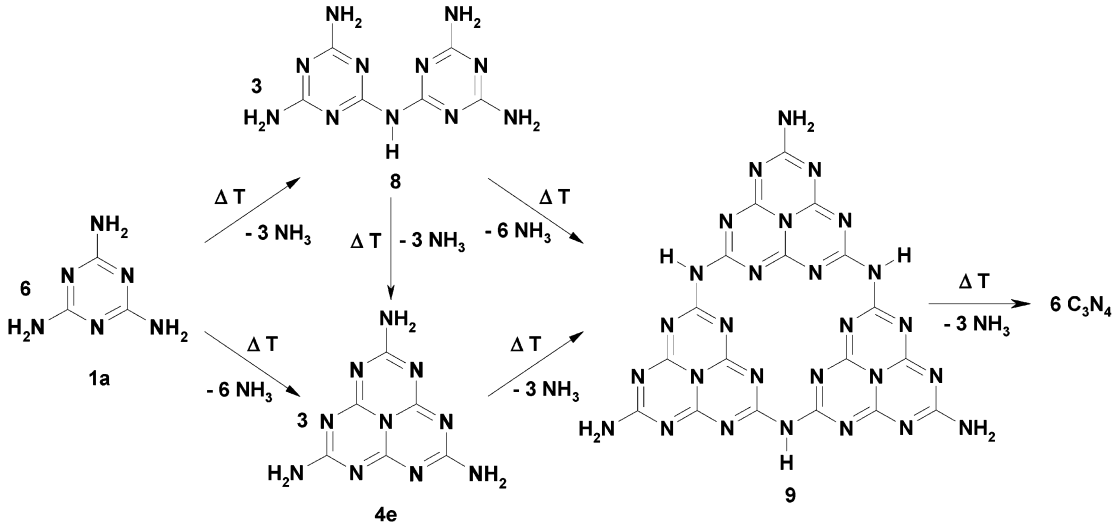

Herein, we report on the synthesis of melem **4e** obtained in preparative amounts, its crystal structure determination, and spectroscopic investigation. Thus, we confirm the existence of a fundamental C−N−H molecule, that has been postulated a long time ago.

Experimental Section

Preparation of Melem $C_6N_7(NH_2)_3$. Melem **4e** was synthesized by heating cyanamide **5** (Fluka, ≥98%) or ammonium dicyanamide **6** (for preparation, see ref 24) or dicyandiamide **7** (Avocado, 99%) or melamine **1a** (Fluka, purum, ≥99% (NT)). The commercial products were used as purchased: 80 mg of starting material (1.90 mmol of **5**, 0.95 mmol of **6**, 0.95 mmol of **7**, or 0.63 mmol of **1a**, respectively) was filled into a glass ampule (outer diameter, 16 mm; inner diameter, 12 mm). The ampule was sealed at a length of 120 mm and heated to 450 °C (heating rate: 1 °C min^{-1}). After about 5 h at this temperature, the ampule was slowly (2 °C min^{-1}) cooled to room temperature.

After the ampule was opened, the typical smell of ammonia was detected. At the top of the ampule, colorless crystals were found which were identified by X-ray powder diffractometry as sublimated melamine. At the bottom, a white-beige powder containing melem was isolated. The product has formed with a yield of ca. 60%. It is not moisture sensitive. Anal. calcd for melem: H, 2.75; C, 33.03; N, 64.22. Found: H, 2.98; C, 32.62; N, 62.04.

Preparation of ^{15}N-Enriched Samples of Melamine and Melem. For ^{15}N MAS NMR investigations, a special synthesis was developed to prepare ^{15}N-enriched samples: 54.4 mg (0.20 mmol) of $Na_3[C_6N_9]$ (for preparation, see ref 33) was heated with 15.1 mg (0.28 mmol) of sublimated $^{15}NH_4Cl$ (Promochem, 98 at. % enriched) under argon up to 470 °C (heating rate: 1 °C min^{-1}) in a sealed glass ampule (outer diameter, 16 mm; inner diameter, 12 mm; length, 120 mm). After the mixture was cooled, NaCl as well as a yellow insoluble polymer remained at the bottom of the ampule. At the top, a beige reaction product was found containing melamine. Subsequent sublimation (220 °C, 1 Pa) of this product leads to nearly pure melamine with a significantly higher content of ^{15}N within both the amino groups and the *s*-triazine ring.

Samples of $C_3{}^{15}N_3(^{15}NH_2)_3$ were used to prepare ^{15}N-enriched melem $C_6{}^{15}N_7(^{15}NH_2)_3$, which contains ^{15}N atoms within the tri-*s*-triazine ring as well as within the amino groups.

Physical Measurements. X-ray Diffraction. X-ray powder diffraction data were used for the crystal structure determination because no single crystals of melem were available. The microcrystalline samples were enclosed in glass capillaries of diameter 0.3 mm. The diffraction investigations were carried out in Debye−Scherrer geometry. The diffraction data were collected on a conventional powder diffractometer (STOE Stadi P, Cu Kα_1 radiation).

Temperature-dependent X-ray powder diffraction experiments were performed on a STOE Stadi P powder diffractometer (Mo Kα_1) with a computer controlled STOE furnace: Samples of melamine and of melem, respectively, were enclosed in silica capillaries and heated from room temperature to 700 °C in the angular range $3° \leq 2\theta \leq 30°$. Powder diffraction patterns were recorded in steps of 20 °C. Additionally, a sample of melem was cooled with a 600 Series Cryostream Cooler (Oxford Cryosystems) from room temperature to −140 °C. The cooling procedure was interrupted in steps of 20 °C to record diffraction patterns at constant temperatures.

Thermoanalytical Investigations. A DSC curve of melamine was recorded with a DSC 141 (Setaram): 17.906 mg (0.142 mmol) of melamine **1a** was filled under argon into a steel pressure crucible and heated to 500 °C (heating rate: 5 °C min^{-1}). Additionally, the thermal effects during cooling were recorded. The use of special pressure

(32) Varghese, J. N.; O'Connell, A. M.; Maslen, E. N. *Acta Crystallogr.* **1977**, *B33*, 2102.
(33) Jürgens, B.; Irran, E.; Schneider, J.; Schnick, W. *Inorg. Chem.* **2000**, *39*, 665.

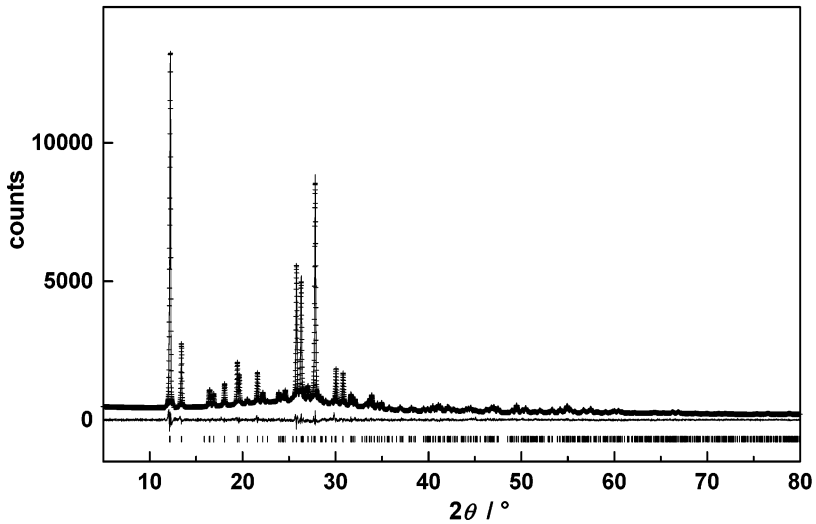

Figure 1. Observed (crosses) and calculated (line) X-ray powder diffraction patterns as well as difference profiles of the Rietveld refinement of melem **4e** (STOE Stadi P, $\lambda = 154.06$ pm).

crucibles was necessary because conventional alumina crucibles burst due to evolution of ammonia.

Solid-State MAS NMR Spectroscopy. ^{13}C and ^{15}N MAS NMR spectra of melamine and melem were recorded at room temperature with a conventional impulse spectrometer DSX 500 Avance (Bruker) operating at 500 MHz. For recording the ^{15}N MAS NMR spectra, ^{15}N-enriched samples of both compounds were used.

The samples were filled into zirconia rotors with a diameter of 4 mm and mounted in a standard double-resonance MAS probe (Bruker). The signals were referenced to trimethylsilane (TMS) (^{13}C) and nitromethane (^{15}N), respectively. Rotation frequencies between 3 and 7 kHz were chosen.

A ramped cross-polarization sequence was employed to excite both ^{13}C and ^{15}N nuclei via the proton bath where the power of the ^{1}H radiation was linearly varied about 50%. A CPPI (cross-polarization combined with polarization inversion) experiment was performed to investigate the bonding and the position of the hydrogen atoms of melamine and melem, respectively. For these experiments, rotation frequencies of 3.7 kHz (melamine) and 5 kHz (melem) and an initial contact time of 30 ms before inverting the sign of the ^{1}H radiation were used. The data collection of all experiments was performed applying broadband proton decoupling via a TPPM sequence.[34]

Vibrational Spectroscopy. FTIR spectra of melamine and melem were obtained at room temperature by using a Bruker IFS 66v/S spectrometer with DTGS detector. The samples were thoroughly mixed with dried KBr (5 mg of sample, 500 mg of KBr). The preparation procedures were performed in a glovebox under dried argon atmosphere. The spectra were collected in a range from 400 to 4000 cm^{-1} with a resolution of 2 cm^{-1}. During the measurement, the sample chamber was evacuated.

For FT-Raman measurements, samples of melamine and melem were filled into glass capillaries of 0.5 mm diameter. The spectra were excited by a Bruker FRA 106/S module with a Nd:YAG laser ($\lambda = 1064$ nm) scanning a range from 0 to 3500 cm^{-1}.

Photoluminescence Spectroscopy. Photoluminescence spectra were recorded with a spectrofluorimeter FL900 (Edinburgh Instruments) with a Xe lamp as the light source and a Hamamatsu photomultiplier. $BaMgAl_{10}O_{17}$:Eu which has a quantum efficiency of 90% at 254 nm was used as reference. The transfer function of the spectrometer has been calibrated over the entire frequency range of the measurements utilizing reference phosphors.

Mass Spectrometry. Mass spectra were obtained with a JEOL MStation JMS 700. The source was operated at a temperature of 200 °C.

Calculations. Methods. The theoretical assessment of the structural properties of $C_6N_7(NH_2)_3$ is based on a detailed comparison of computational results for both the molecular and the extended state. The molecular-orbital calculations were performed using the Gaussian quantum chemistry software package.[35] Beckes three-parameter hybrid functional (B3LYP)[36,37] was employed as well as the second-order Møller−Plesset perturbation theory (MP2).[38] Dunning's correlation-consistent basis set (cc-pVDZ) was used.[39] A Pople-type basis set (6-311++G**) yielded very similar results.

The structural optimizations in the extended state were done using the Vienna ab initio simulation package (VASP).[40−43] Ultrasoft pseudopotentials were employed for the atoms, and the exchange-correlation energy of the valence electrons was treated at the DFT level using both the local density approximation (LDA)[44] and the generalized-gradient approximation (GGA).[45] The wave function was expanded into a plane wave basis set using a cutoff energy of 400 eV; for the integration over the Brillouin Zone, a Monkhorst−Pack $2 \times 2 \times 2$ k-point mesh was used.[46] Initial positions of atoms were the crystal coordinates supplied by the refinement of the X-ray diffraction data. During relaxation, all crystal coordinates were optimized while keeping space group symmetry and experimental lattice constants fixed. Releasing the latter constraint showed the usual trends of LDA and GGA tending to smaller and larger volumes, each by 4%, respectively.

(34) Bennett, A. E.; Rienstra, C. M.; Auger, M.; Lakshimi, K. V.; Griffin, R. G. *J. Chem. Phys.* **1995**, *103*, 6951.
(35) Frisch, M. J.; Trucks, G. W.; Schlegel, H. B.; Scuseria, G. E.; Robb, M. A.; Cheeseman, J. R.; Zakrzewski, V. G.; Montgomery, J. A., Jr.; Stratmann, R. E.; Burant, J. C.; Dapprich, S.; Millam, J. M.; Daniels, A. D.; Kudin, K. N.; Strain, M. C.; Farkas, O.; Tomasi, J.; Barone, V.; Cossi, M.; Cammi, R.; Mennucci, B.; Pomelli, C.; Adamo, C.; Clifford, S.; Ochterski, J.; Petersson, G. A.; Ayala, P. Y.; Cui, Q.; Morokuma, K.; Malick, D. K.; Rabuck, A. D.; Raghavachari, K.; Foresman, J. B.; Cioslowski, J.; Ortiz, J. V.; Stefanov, B. B.; Liu, G.; Liashenko, A.; Piskorz, P.; Komaromi, I.; Gomperts, R.; Martin, R. L.; Fox, D. J.; Keith, T.; Al-Laham, M. A.; Peng, C. Y.; Nanayakkara, A.; Gonzalez, C.; Challacombe, M.; Gill, P. M. W.; Johnson, B. G.; Chen, W.; Wong, M. W.; Andres, J. L.; Head-Gordon, M.; Replogle, E. S.; Pople, J. A. *Gaussian 98*, revision A.11; Gaussian, Inc.: Pittsburgh, PA, 1998.
(36) Becke, A. D. *Phys. Rev. A* **1988**, *38*, 3098.
(37) Lee, C.; Yang, W.; Parr, R. G. *Phys. Rev. B* **1988**, *37*, 785.
(38) Møller, C.; Plesset, M. S. *Phys. Rev.* **1934**, *46*, 618.
(39) Dunning, T. H. *J. Chem. Phys.* **1989**, *90*, 1007.
(40) Kresse, G.; Hafner, J. *Phys. Rev. B* **1993**, *47*, 558.
(41) Kresse, G.; Hafner, J. *Phys. Rev. B* **1994**, *49*, 14251.
(42) Kresse, G.; Furthmüller, J. *Comput. Mater. Sci.* **1996**, *6*, 15.
(43) Kresse, G.; Furthmüller, J. *Phys. Rev. B* **1996**, *54*, 11169.
(44) Perdew, J. P.; Zunger, A. *Phys. Rev. B* **1981**, *23*, 5048.
(45) Perdew, J. P. In *Electronic Structure of Solids '91*; Eschrig, P. H., Ed.; Akademie Verlag: Berlin, 1991.
(46) Monkhorst, H. J.; Pack, J. D. *Phys. Rev. B* **1976**, *13*, 5188.

Table 1. Crystallographic Data for Melem $C_6N_7(NH_2)_3$

formula	$H_6C_6N_{10}$
M_r/g mol^{-1}	218.18
crystal system	monoclinic
space group	$P2_1/c$ (no. 14)
powder diffractometer	Stoe STADI P
radiation; λ/pm	Cu Kα_1; 154.06
temperature/°C	22
lattice parameters	
a/pm	739.92(1)
b/pm	865.28(3)
c/pm	1338.16(4)
β/deg	99.912(2)
$V/10^6$ pm^3	843.95(4)
Z	4
ρ_{calc}/g cm^{-3}	1.717
profile range	$5° \le 2\theta \le 80°$
no. of data points	7500
observed reflections	515
structural parameters	68
profile parameters	18
χ^2	0.883
structure refinement	Rietveld refinement (GSAS)[47]
R-values	
wR_p	0.056
R_p	0.042
R_F	0.079

Results and Discussion

Powder Diffractometry and Structure Refinement. The diffraction pattern of a room-temperature measurement of melem was indexed with a monoclinic unit cell (Figure 1, Table 1). The extinction rules unequivocally indicated the space group $P2_1/c$. A structure solution with direct methods was not possible. To solve the structure, the profile and lattice constants were refined by the LeBail method. For these calculations and also for the Rietveld refinement, the program GSAS was employed.[47] The crystal structure was solved by a combination of trial-and-error and rigid-body methods. The atomic positions of the molecule neglecting the outermost NH_2 groups were calculated in a random position in the unit cell. The distances between the atoms were restrained with a very high weight, so that nearly a rigid body was formed. As a reference for the atomic distances, the data of $C_6N_7Cl_3$ **4d** were taken from Kroke et al.[17] The positions of all atoms were refined simultaneously. When the refinement reached a local minimum ($R_{F^2} \approx 60\%$), the weight of the restraints was reduced to zero, and therefore the atoms randomized and were released to positions of high electron density. The weight was then increased again so the molecule was formed again. This procedure was repeated twice, and then the molecule reached a position where it gave a low R_{F^2} value (~20%). Refinement with a low weight gave an R-value of about 15%. A subsequent Fourier map clearly revealed the positions of the N atoms of the outermost NH_2 groups. This result nicely illustrates the reliability of the position and orientation of the melem molecule in the cell. The H atoms of the NH_2 groups could not be found by difference Fourier synthesis. Their positions were calculated by the program SHELX[48] and refined with restraints. Details of the structure determination and refinement are listed in Table 1, and the refined atomic coordinates are given in Table 2. In Scheme 5, the labeling of the different C and N positions of the melem molecule is illustrated.

Table 2. Atomic Coordinates and Displacement Factors (in pm^2) for Melem $C_6N_7(NH_2)_3$; All Atoms in Wyckoff Position 4*e*

atom	x	y	z	U_{iso}[a]
C(i)1	0.765(2)	0.203(2)	0.447(1)	440(20)
C(i)2	0.675(2)	−0.069(2)	0.453(1)	440(20)
C(i)3	0.867(2)	0.046(2)	0.593(1)	440(20)
C(e)4	0.602(2)	0.093(1)	0.3119(9)	440(20)
C(e)5	0.773(2)	−0.195(1)	0.5924(9)	440(20)
C(e)6	0.959(2)	0.294(1)	0.5903(8)	440(20)
N(i)1	0.771(1)	0.065(2)	0.5019(9)	320(10)
N(c)2	0.695(1)	0.221(1)	0.3509(7)	320(10)
N(c)3	0.581(1)	−0.044(1)	0.3644(8)	320(10)
N(c)4	0.659(1)	−0.196(1)	0.5017(8)	320(10)
N(c)5	0.870(1)	−0.083(1)	0.6515(9)	320(10)
N(c)6	0.956(1)	0.169(1)	0.6443(8)	320(10)
N(c)7	0.883(1)	0.315(1)	0.4956(7)	320(10)
N(t)8	0.511(1)	0.1046(8)	0.2226(6)	320(10)
N(t)9	0.766(1)	−0.3282(9)	0.6460(7)	320(10)
N(t)10	1.056(1)	0.413(1)	0.6356(7)	320(10)
H1	0.542(5)	0.164(4)	0.183(1)	250
H2	0.427(3)	0.047(3)	0.204(1)	250
H3	0.679(4)	−0.384(4)	0.633(2)	250
H4	0.846(3)	−0.349(2)	0.692(2)	250
H5	1.081(5)	0.416(2)	0.696(7)	250
H6	1.091(4)	0.479(2)	0.602(1)	250

[a] U_{iso} is defined as $\exp(-8\pi^2 U_{iso} \sin^2\theta/\lambda^2)$; U_{iso} values of H atoms are not refined.

Scheme 5. One Melem Molecule in the Crystal Structure of $C_6N_7(NH_2)_3$[a]

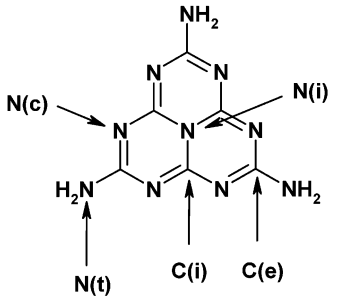

[a] The labeling of the atoms is indicated. The molecule adopts approximately symmetry D_{3h}.

Crystal Structure. Solid melem **4e** consists of $C_6N_7(NH_2)_3$ molecules interconnected by extended hydrogen bridges. Comparable to the situation found in tri-*s*-triazine and trichloro-tri-*s*-triazine, each molecule contains a cyameluric nucleus C_6N_7 of three anellated *s*-triazine rings. In the case of melem, the structure is completed by three terminal N atoms bound to positions 2, 5, and 8 of the tri-*s*-triazine C_6N_7 nucleus.

In the asymmetric unit, there is one complete $C_6N_7(NH_2)_3$ molecule (Figure 2). Two differently orientated layers of parallel molecules alternate along the direction of the *c*-axis. The planes of the planar molecules are slightly tilted to the (10-1) plane. Layers of $C_6N_7(NH_2)_3$ molecules are formed which are parallel to this plane. Neighboring molecules form an angle of about 40°. The interlayer distance is 327 pm. This value is comparable to the respective distances in melamine (320 pm − 340 pm), in the C−N polymer $[C_6N_9H_4]Cl$ (322 pm), as well as in pure graphite (334 pm). The relatively short interlayer distance observed in melem may be explained by intermolecular $\pi\cdots\pi$ interactions between the aromatic C_6N_7 nuclei.

The ring system of $C_6N_7(NH_2)_3$ is quite planar; the sums of the bond angles around each atom are 360°. The rings are

(47) Larson, A. C.; von Dreele, R. B. General Structure Analysis System, Los Alamos National Laboratory Report LAUR 86-748, 1990.
(48) Sheldrick, G. M. *SHELXTL, V 5.10 Crystallographic System*; Bruker AXS Analytical X-ray Instruments Inc.: Madison, 1997.

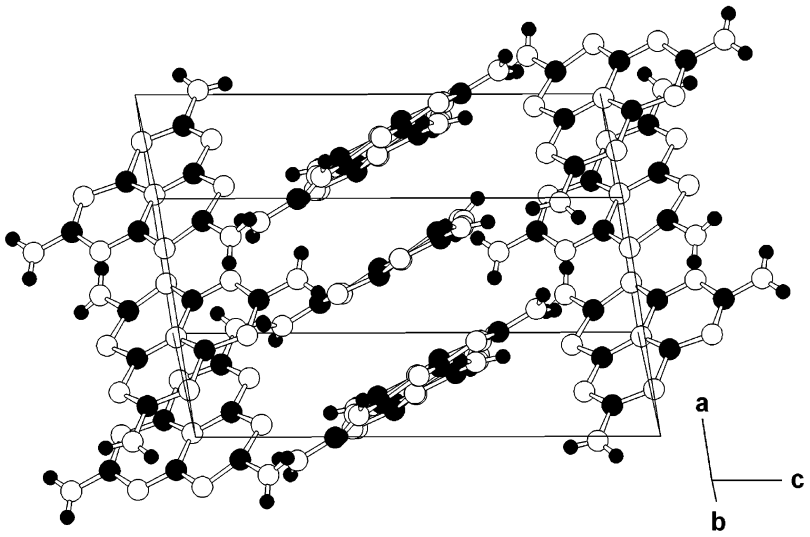

Figure 2. Crystal structure of melem **4e**.

Table 3. Atomic Distances (in pm) and Angles (in deg) in $C_6N_7(NH_2)_3$ (Distances N(t)−H and Angles C(e)−N(t)−H and H−N(t)−H Are Constrained)

C(i)1−N(i)1	139(2)	N(i)1−C(i)1−N(c)2	126(2)	C(i)1−N(i)1−C(i)2	118(2)
C(i)1−N(c)2	131(1)	N(i)1−C(i)1−N(c)7	113(2)	C(i)1−N(i)1−C(i)3	124(2)
C(i)1−N(c)7	139(1)	N(c)2−C(i)1−N(c)7	119(2)	C(i)2−N(i)1−C(i)3	117(1)
C(i)2−N(i)1	146(2)	N(i)1−C(i)2−N(c)3	115(1)	C(i)1−N(c)2−C(e)4	111(1)
C(i)2−N(c)3	128(2)	N(i)1−C(i)2−N(c)4	122(1)	C(i)2−N(c)3−C(e)4	121(1)
C(i)2−N(c)4	130(2)	N(c)3−C(i)2−N(c)4	122(2)	C(i)2−N(c)4−C(e)5	110(1)
C(i)3−N(i)1	132(2)	N(i)1−C(i)3−N(c)5	127(2)	C(i)3−N(c)5−C(e)5	107(1)
C(i)3−N(c)5	135(1)	N(i)1−C(i)3−N(c)6	120(1)	C(i)3−N(c)6−C(e)6	115(1)
C(i)3−N(c)6	137(2)	N(c)5−C(i)3−N(c)6	113(1)	C(i)1−N(c)7−C(e)6	119(1)
C(e)4−N(c)2	136(1)	N(c)2−C(e)4−N(c)3	126(1)		
C(e)4−N(c)3	140(1)	N(c)2−C(e)4−N(t)8	117(2)		
C(e)4−N(t)8	127(1)	N(c)3−C(e)4−N(t)8	117(2)		
C(e)5−N(c)4	135(2)	N(c)4−C(e)5−N(c)5	135(1)		
C(e)5−N(c)5	138(1)	N(c)4−C(e)5−N(t)9	113(2)		
C(e)5−N(t)9	136(1)	N(c)5−C(e)5−N(t)9	111(2)		
C(e)6−N(c)6	130(1)	N(c)6−C(e)6−N(c)7	128(1)		
C(e)6−N(c)7	131(2)	N(c)6−C(e)6−N(t)10	116(2)		
C(e)6−N(t)10	134(1)	N(c)7−C(e)6−N(t)10	116(2)		

distorted in a way similar to that in tri-*s*-triazine **4c**[20] and trichloro-tri-*s*-triazine **4d**.[17] The average distance between N(i)1 and the neighboring C(i) atoms (139 pm) is slightly longer than the average distances of C(i)−N(c) (133 pm) and C(e)−N(c) (135 pm) within the cyameluric ring. As is also found in tri-*s*-triazine and trichloro-tri-*s*-triazine, the average angle N(c)−C(e)−N(c) of the ring system is larger (130°), and the average C(i)−N(c)−C(e) angle is smaller than 120° (114°), while all other average angles are 120°. The deviations of the individual distances and angles (Table 3) from the average values can be explained by the lower accuracy of the X-ray powder diffractometry as compared to single-crystal structure determinations. Nevertheless, it is quite remarkable that, on the basis of conventional powder diffraction data, a relatively complex structure could be solved and refined unambiguously (large cell volume of 844×10^6 pm^3, 16 atoms in the asymmetric unit, 68 structural and 18 profile parameters) without the use of a high-resolution diffraction experiment.

The average distance between the C(e) atoms and the N(t) atoms of the NH_2 groups is 132 pm, which is in the range of the corresponding distances found in melamine.[31,32] The crystallographic point symmetry of the molecule is C_1, although it comes close to D_{3h}.

As the position of the H atoms could not be obtained experimentally, hydrogen bonds cannot be identified unambiguously. However, there are three intermolecular distances N···N which are in the range of the hydrogen bonds found in melamine. The first two intermolecular distances N(c)5−N(t)10 and N(c)6−N(t)9 amount to 285(2) and 317(1) pm, respectively. Thus, they are predestined for hydrogen bonding. The two hydrogen bonds mentioned above connect neighboring molecules within one layer parallel (10-1). Furthermore, a third hydrogen bond is formed from N(t)10 with a short intermolecular distance of 300(2) pm to a N(c)7 atom of a melem molecule within a different layer. For N(t)8, a hydrogen bond to N(c)3 can be assumed because of the distance N(t)8−H···N(c)3 of 328 pm. Altogether, there are eight hydrogen bonds per $C_6N_7(NH_2)_3$ molecule (Figure 3). Thus, there are as many hydrogen bonds as were found in melamine. In the latter, four pairs of parallel hydrogen bonds between the molecules occur.

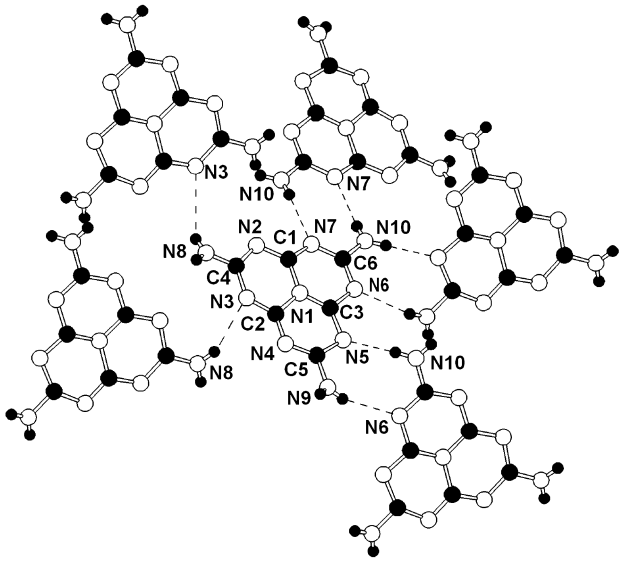

Figure 3. Hydrogen bonds between melem molecules. The molecules in the middle and top right belong to the same layer.

According to temperature-dependent X-ray diffractometry within the temperature range from −140 to 520 °C, the lattice parameters steadily increase (*a* 5.7%, *c* 3.9%, *β* 2.4%). In contrast, parameter *b* is nearly constant with only a minor increase of 1.4%.

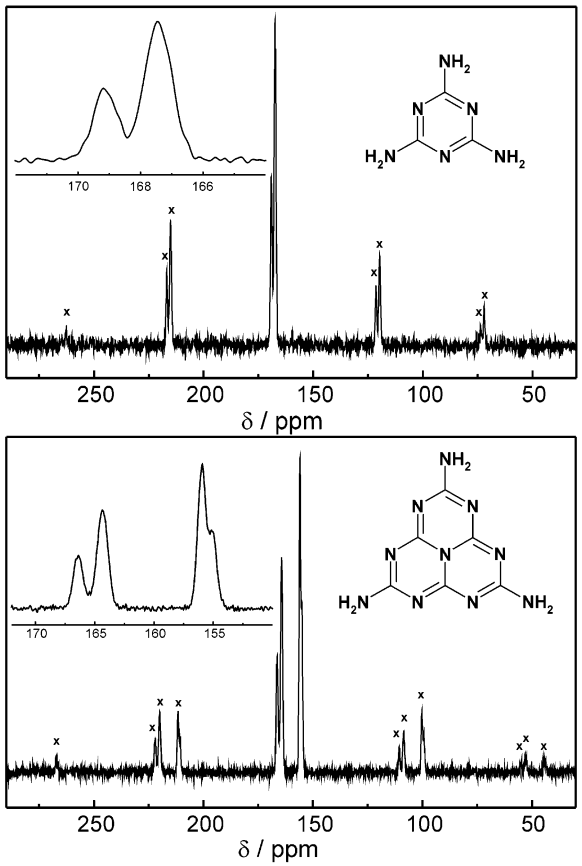

Figure 4. ^{13}C MAS NMR spectra of melamine **1a** (top) and melem **4e** (bottom). ×'s indicate spinning sidebands.

Solid-State MAS NMR Characterization. ^{13}C MAS NMR Spectroscopic Characterization. The ^{13}C MAS NMR spectrum of melamine (Figure 4) reveals two signals in a 1.9(1):1 intensity ratio at 167.5 and 169.2 ppm. Normally, cross-polarization experiments are not reliable for quantitative intensity analysis, but they give a rough clue for the number of atoms which cause a signal. The observed shifts are slightly different from those reported by Damodaran et al. who found a similar intensity ratio for signals at 166.2 and 167.8 ppm.[49] In melamine dissolved in DMSO, the carbon atoms become magnetically equivalent, and only one shift is observed at 167.1 ppm.[50] The observed values are in good agreement with those found for sp^2-hybridized carbon atoms in the *s*-triazine ring systems of other carbon nitride materials.[7,10] An overview of the observed chemical shifts for melamine and melem is given in Scheme 6.

The ^{13}C MAS NMR spectrum of melem (Figure 4) exhibits two signal groups. The resonances for the $C(e)N_2(NH_2)$ groups observed at 164.3 and 166.4 ppm with a 1.9(1):1 intensity ratio are comparable to those found for melamine. In contrast, the carbon atoms CN_2X (X = H, Cl) in tri-*s*-triazine and 2,5,8-trichloro-tri-*s*-triazine are shifted to higher values (171.6 ppm in $C_6N_7H_3$[21] and 175.0 ppm in $C_6N_7Cl_3$[17]). The second signal group in the spectrum of melem belongs to the $C(i)N_3$ groups of the cyameluric nucleus: These are observed at 155.1 and 156.0 ppm, which are comparable to the signals found for $C_6N_7H_3$ (159.7 ppm)[21] and $C_6N_7Cl_3$ (158.2 ppm).[17]

Scheme 6. ^{13}C and ^{15}N Chemical Shifts Observed for Melamine **1a** and Melem **4e**

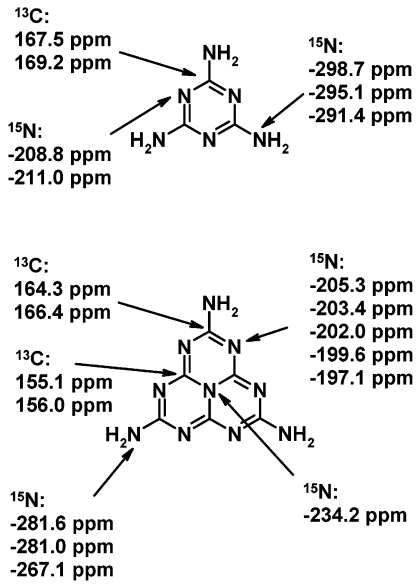

^{15}N MAS NMR Spectroscopic Characterization. A ^{15}N MAS NMR spectrum of melamine in natural abundance was performed by Damodaran et al. The authors observed resonances at 83.9, 87.4, 90.9, 171.6, and 173.7 ppm (referenced to liquid ammonia) according to values at −296.3, −292.8, −289.3, −208.6, and −206.5 ppm (referenced to nitromethane).[49]

In this work, a ^{15}N MAS NMR spectrum of ^{15}N (>90%)-enriched melamine was recorded (Figure 5, Scheme 6). In the spectrum, resonances of the three amino groups are observed at −298.7, −295.1, and −291.4 ppm. The signals at −211.0 and −208.8 ppm with a 2.0(2):1 intensity ratio are assigned to the ring N atoms of the *s*-triazine ring. These results are in agreement with those found by Damodaran et al. for melamine as well as for those of substituted triamino-*s*-triazines.[51]

The signals of the ring N atoms of nonsubstituted *s*-triazine $C_3N_3H_3$ dissolved in DMSO are observed at −98.5 ppm.[52] The significant difference of about 110 ppm between the shifts found for the N ring atoms of *s*-triazine and melamine is caused presumably by the influence of the three amino groups in melamine. The same influence of amino groups is observed for tri-*s*-triazine and the respective triamino-substituted derivative melem: In the ^{15}N MAS NMR spectrum of tri-*s*-triazine dissolved in DMSO, the ring N atoms are observed at 133.8 ppm (referenced to DMF) which corresponds to −141.4 ppm (referenced to nitromethane).[21]

The amino groups of melem provide a significant shift to lower values: In the ^{15}N MAS NMR spectrum of melem, resonances of the N(c) atoms within the cyameluric ring are observed at −197.1, −199.6, −202.0, −203.4, and −205.3 ppm with intensity ratios of 1:1.0(1):1.1(1):1.2(1):2.3(1). The intensities indicate the presence of six N(c) atoms within the cyameluric nucleus. Even for the central atom N(i), the influence of the amino groups is observed: In tri-*s*-triazine, the shift of the central ^{15}N atom is found at 81.8 ppm (referenced to DMF) or −193.4 ppm (referenced to nitromethane). In the triamino

(49) Damodaran, K.; Sanjayan, G. J.; Rajamohanan, P. R.; Ganapathy, S.; Ganesh, K. N. *Org. Lett.* **2001**, *3*, 1921.
(50) Pouchert, C. J. *The Aldrich Library of NMR Spectra*, 2nd ed.; Aldrich Chemical Co.: Milwaukee, WI, 1983.
(51) Amm, M.; Platzer, N.; Guilhem, J.; Bouchet, J. P.; Volland, J. P. *Magn. Reson. Chem.* **1998**, *36*, 587.
(52) Stefaniak, L.; Roberts, J. D.; Witanowski, M.; Webb, G. A. *Org. Magn. Reson.* **1984**, *22*, 201.

Scheme 7. Possible Tautomers of Melamine **1a** and Melem **4e**

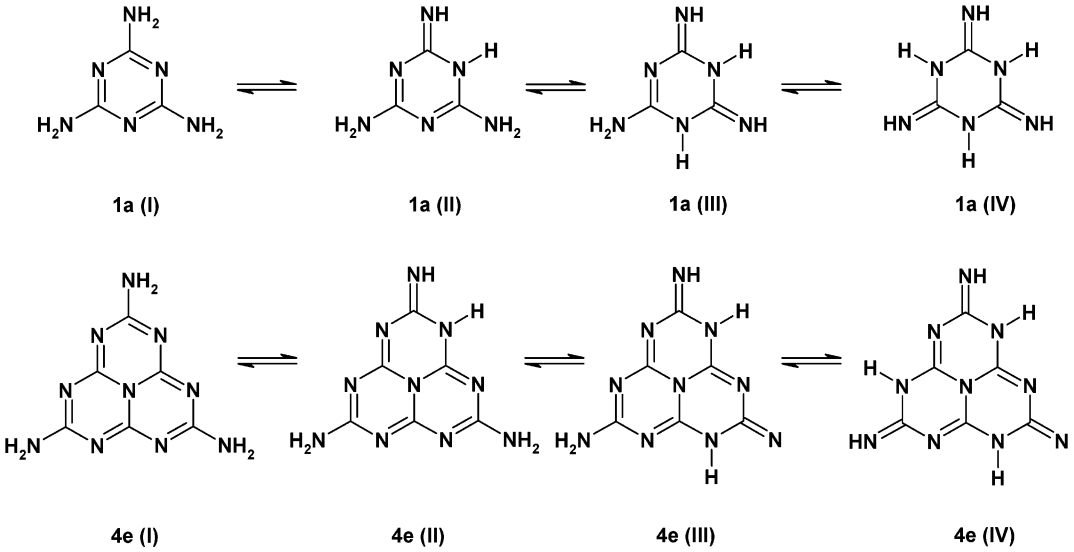

derivative melem, the resonance is observed at −234.4 ppm. The lowest shifts in the ^{15}N MAS NMR spectrum of melem are caused by the amino groups at −267.1, −281.0, and −281.6 ppm.

CPPI (Cross-Polarization Combined with Polarization Inversion) Experiment. For melamine as well as for melem, the occurrence of different tautomeric forms seems to be possible (Scheme 7). In the case of melamine, the presence of tautomer **1a**(I) was confirmed by X-ray and neutron diffraction.[31,32]

For melem **4e**, a localization of the H atoms by X-ray powder diffractometry was not possible. To determine which tautomer **4e**(I)−(IV) occurs in the solid, a CPPI experiment was recorded.[53,54] This modified CP sequence allows one to differentiate various N sites due to the existence of NH_2 and NH groups as well as of tertiary N atoms carrying no proton. During the sequence, the magnetization starts from an optimum value. It decreases and becomes negative with increasing inversion time.[53,54] The descent of the normalized intensities by increasing inversion times can be described by eq 1.

$$M_s(t_i) = M_o(t_C)\left[\frac{2}{n+1}\exp\left(-\frac{t_i}{T_D}\right) + \frac{2n}{n+1}\exp\left(-\frac{3t_i}{2T_D}\right) + \left(-\frac{{t_i}^2}{{T_C}^2}\right) - 1\right] \quad (1)$$

The parameter n characterizes the number of protons which are directly bound to the N atoms. T_C is related to dipolar coupling to nearby protons leading to a coherent transfer of polarization, while T_D describes the decay caused by isotropic spin diffusion ($T_C \ll T_D$).

The experimental polarization inversion curves for melamine and melem are given in Figure 6. The intensity of all resonances is normalized with respect to their intensities for $t_i = 0$. Thus, the starting point of the resulting hyperbola is 1 in all cases of n ($n = 0, 1, 2$) given in eq 1. In the first hundred microseconds, the intensity decreases rapidly because of the transfer of magnetization to nearby protons. In a second time-regime, the curve decreases with a much slower rate due to spin diffusion. The crossover of the normalized intensity is observed at $[2/(n+1)] - 1$ corresponding to $\exp(-3t_i^2/T_C^2)$ ($t_i \gg T_C$) and $\exp(-t_i/T_D) \approx 1$ ($t_i \ll T_D$). In the case of $n = 1$, the crossover region is expected at 0; for $n = 2$, it should occur at $-1/3$.

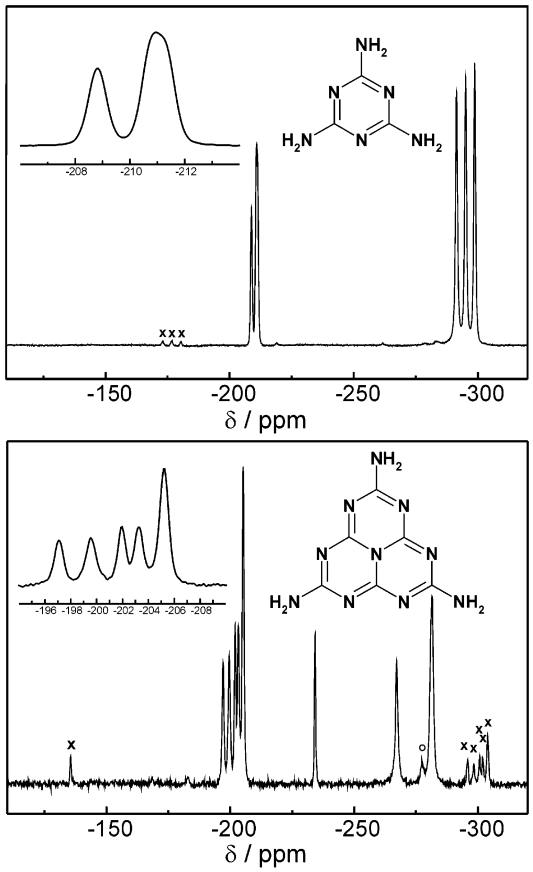

Figure 5. ^{15}N MAS NMR spectra of melamine **1a** (top) and melem **4e** (bottom). ×'s indicate spinning sidebands; an impurity is marked with ○.

(53) Gervais, C.; Maquet, J.; Babonneau, F.; Duriez, C.; Framery, E.; Vaultier, M.; Florian, P.; Massiot, D. *Chem. Mater.* **2001**, *13*, 1700.
(54) Gervais, C.; Babonneau, F.; Maquet, J.; Bonhomme, C.; Massiot, D.; Framery, E.; Vaultier, M. *Magn. Reson. Chem.* **1998**, *36*, 407.

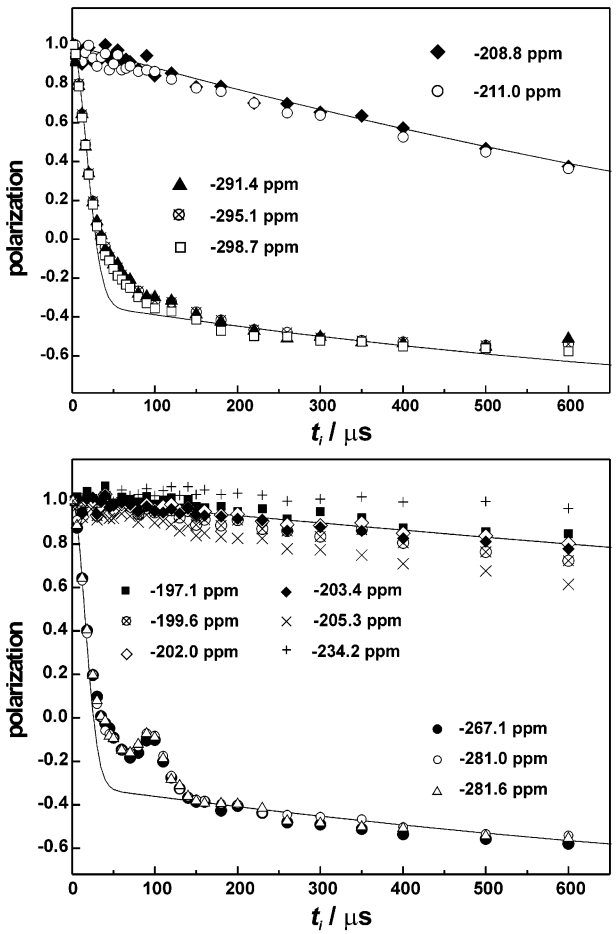

Figure 6. Normalized signal intensities versus inversion time t_i of the ^{15}N CPPI MAS NMR experiments for melamine **1a** (upper graph) and melem **4e** (lower graph).

To test the significance of a CPPI experiment for the structure determination of melem, this experiment was first applied to melamine which unequivocally crystallizes in the amino form[31,32] (Scheme 7). Thus, in the case of melamine, two different cases of polarization decays are to be expected. Because no hydrogen atom is covalently bound to the ring atoms, a slow polarization decay should occur for these resonances at both short and long t_i. For the nitrogen atoms with two hydrogen atoms covalently bound ($n = 2$), the polarization is rapidly transferred back to the protons for small t_i. For larger t_i, the polarization transfer mechanism changes to spin diffusion, and, therefore, a crossover to a slow decay will be observed at a polarization of $-1/3$. The experimental CPPI curves for melamine are in excellent agreement with these conclusions. The polarization of the nuclei with $\sigma_{iso} = -208.8$ and -211.0 ppm decreases slowly without a crossover section, whereas for the polarization of the nuclei with $\sigma_{iso} = -291.4$, -295.1, -298.7 ppm, a crossover is observed at -0.3. Consequently, the former and the latter resonances unambiguously can be assigned to the nitrogen atoms in the ring and the amino groups, respectively.

The curves for melem are comparable: The respective curves of the six resonances at -234.2, -205.3, -203.4, -202.0, -199.6, and -197.1 ppm decrease quite slowly. These correspond to the seven nonprotonated N(c) atoms within the cyameluric nucleus. Furthermore, the curves of the resonances at -267.1, -281.0, and -281.6 ppm exhibit behavior similar to those of the NH_2 groups of melamine, as they have a crossover nearby -0.3. No curve is found with a crossover region at about 0, thus indicating that no imido N atoms occur in the molecule. Therefore, the tautomer **4e**(I) describes the correct bonding situation as well as the existence of three amino groups in melem.

For the resonances which represent the ring N(c) atoms, different parameters T_D are observed which can be divided into three groups. For the resonances at -197.1 and -202.0 ppm, the longest T_D values ($\sim$6.0 ms) are observed. For the signals at -199.6 and -203.4 ppm, T_D values were determined to be 4.4 and 4.9 ms. The shortest time constants ($T_D \approx 3.1$ ms) are found for the two N(c) atoms represented by the resonance at -205.3 ppm. According to the theory outlined above, the magnitude of T_D is influenced by the strength of proton nitrogen contacts. The shorter the closest $^1H^{15}N$ contact is, the smaller the time constant T_D becomes. Thus, the variations of T_D for the resonances mentioned above may now permit an assignment. According to the crystal structure determination, the atoms N(c)5 and N(c)7 are involved in the strongest (shortest) hydrogen bonds. Therefore, the resonance at -205.3 ppm can be assigned to N(c)5 and N(c)7. The observed T_D values are in a range comparable to that of those found in polyborazilene and borane-ammonia complexes by the same CPPI experiment.[53,54]

The resonance at -234.2 ppm has a T_D value of 15 ms; this slow decay indicates the extremely long distance between the N atom and the nearest protons. Therefore, this signal is caused by the N(i)1 atom.

Apart from the results concerning tautomers of melem, the CPPI experiment unequivocally confirms the above-mentioned assignment of the different resonances to the different kinds of N atoms, N(c), N(i), and N(t).

Vibrational Spectroscopic Characterization. According to the general formula $3N - 6$ (N: number of atoms), melem $C_6N_7(NH_2)_3$ has 60 fundamental modes of vibration. These can be divided into two parts: 21 vibrations are associated with the three NH_2 groups of melem, which is comparable to the situation found for melamine with its three amino groups.[55,56] Each NH_2 group has six vibrational modes: the stretching vibrations $\nu_{as}NH_2$ and ν_sNH_2, the bending and rocking vibrations δNH_2 and ρNH_2 which are in-plane, as well as the out-of-plane twisting and wagging vibrations τNH_2 and ωNH_2. The remaining 39 modes are skeletal vibrations belonging to the C_6N_7 nucleus which are found in trichloro-tri-*s*-triazine, too.[17] Apart from the vibrations of the C_6N_7 nucleus and the amino groups in the spectra of melem, vibrations belonging to the three C(e)−N(t)-H_2 groups should appear. In Figure 7, the FTIR and FT-Raman spectra of melem are compared to those of melamine; the observed frequencies and an assignment are given Table 6. In the region above 2800 cm^{-1}, the spectra of both compounds are very similar due to the three amino groups and their respective νN−H stretching vibrations. For the cyameluric nucleus, similar vibrations are expected as found in the IR spectrum of the chlorinated derivative **4d**; for example, the vibrations at 1610 (vs), 1505 (vs), 1310 (vs), and 825 (m) cm^{-1} are observed for **4d**, and signals at 1606 (vs), 1469 (vs), 1304 (m), and 802 (s) are found in the FTIR spectrum of melem **4e**.

(55) Jeremy Jones, W.; Orville-Thomas, W. J. *Trans. Faraday Soc.* **1959**, *55*, 203.
(56) Wang, Y.-L.; Mebel, A. M.; Wu, C.-J.; Chen, Y.-T.; Lin, C.-E.; Jiang, J.-C. *J. Chem. Soc., Faraday Trans.* **1997**, *93*, 3445.

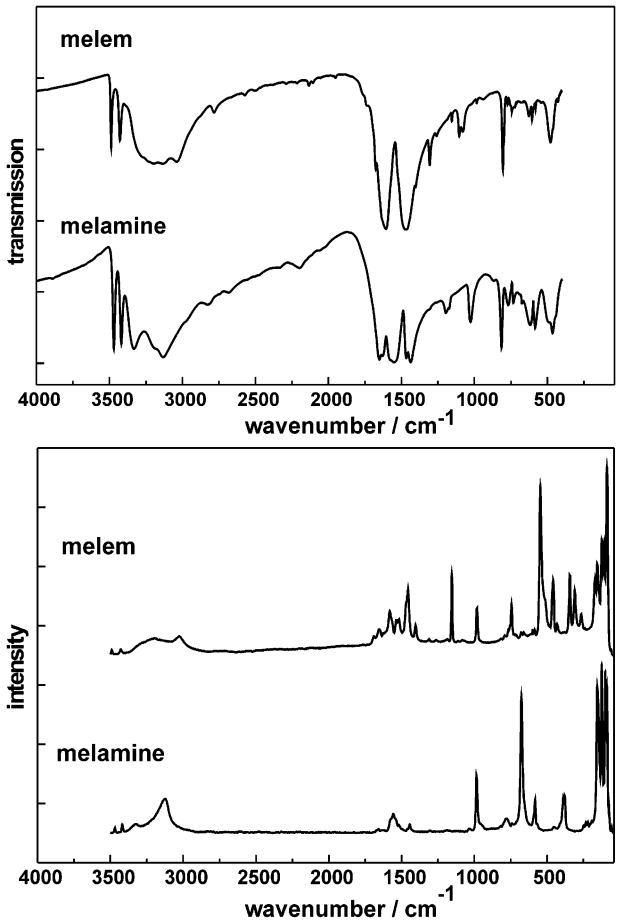

Figure 7. FTIR (upper graph) and FT-Raman (lower graph) spectra of melamine **1a** and melem **4e**.

Table 4. Bond Lengths (in pm) and Angles (in deg) for the Free $C_6N_7(NH_2)_3$ Molecule (Values Are Calculated Using Both DFT (B3LYP Hybrid Functional) and Post-Hartree−Fock Methods (MP2))

bond	B3LYP	MP2
C(i)−N(i)	141.2	141.1
C(i)−N(c)	133.0	133.5
C(e)−N(c)	134.8	135.0
C(e)−N(t)	135.0	135.0
N−H	101.0	101.1
N(c)−C(i)−N(i)	119.6	119.9
N(t)−C(e)−N(c)	115.8	115.5
C(e)−N(c)−C(i)	116.3	115.6
C(i)−N(i)−C(i)	120	120
N(c)−C(i)−N(c)	120.9	120.2
N(c)−C(e)−N(c)	128.3	129.0

Photoluminescence Spectroscopy. In the excitation spectrum of melem, a maximum at $\lambda_{max,\ exc} = 288$ nm ($T = 20$ °C) occurs. The emission spectrum exhibits a maximum at $\lambda_{max,\ emission} =$ 366 nm with a relatively high quantum efficiency of 40% (Figure 8). A significant shift of the emission maximum is observed as compared to the chlorinated derivative **4d** ($\lambda_{max,\ abs} = 310$ nm, $\lambda_{max,\ emission} = 466$ nm).[17]

Mass Spectrometric Characterization. The formula $C_6N_{10}H_6$ of melem was confirmed by mass spectrometry. Apart from the basis peak (*m*/*z* 218) which represents the melem molecule, further fragments are observed. MS (DEI$^+$, 70 eV) *m*/*z*: 219 (MH^+, 10%), 218 (M^+, 100%), 178 ($M^+ - NCN$, 3%), 177 ($M^+ - NCNH$, 33%), 172 ($M^+ - CN_2H_6$, 8%), 135 ($[C_3N_7H]^+$, 4%), 127 ($[C_3N_6H_7]^+$, 5%), 109 ($[C_3N_5H_3]^+$, 5%), 108 ($[C_3N_5H_2]^+$, 7%), 68 ($[C_2N_3H_2]^+$, 21%), 43 ($[CN_2H_3]^+$, 5%), 42 ($[CN_2H_2]^+$, 2%). MS, HR: $C_6N_{10}H_6$: *m*/*z* (calc.) = 218.0777, *m*/*z* (obs.) = 218.0756.

Table 5. Bond Lengths (in pm) and Angles (in deg) for the Calculated Crystal Structure of $C_6N_7(NH_2)_3$[a]

bond	GGA	LDA
C(i)−N(i)	140.6(1)	139.6(1)
C(i)−N(c)	132.7(3)	131.8(3)
C(e)−N(c)	135.6(4)	134.7(5)
C(e)−N(t)	133.3(8)	132.2(9)
N−H	102.7(10)	103.8(15)
N(c)−C(i)−N(i)	119.5(6)	119.3(4)
N(t)−C(e)−N(c)	117.1(10)	117.6(11)
C(e)−N(c)−C(i)	117.6(7)	118.2(5)
C(i)−N(i)−C(i)	120.0 (1)	120.0 (3)
N(c)−C(i)−N(c)	121.0 (2)	121.3 (3)
N(c)−C(e)−N(c)	125.7 (6)	124.8 (8)

[a] The bond lengths and angles are averaged over all chemically identical bonds, with the standared deviation given in parantheses.

Table 6. Calculated Wavenumbers (in cm^{-1}, at the B3LYP/cc-pVDZ Level of Theory) of the $C_6N_7(NH_2)_3$ Molecule in the Gas Phase (Calculated Relative Intensities Truncated to Full Integer Values) in Comparison to Those Found in the Vibrational Spectra of Melem **4e**[a]

$\tilde{\nu}$ **4e** (observed, this work)	$\tilde{\nu}$ **4e** (calculated, this work)	calc. rel intensity		assignment
		IR	Ra	
3488 s (IR), 3498 w (Ra)	3746	99	131	E′
	3746	0	0	A_2'
	3596	0	591	A_1'
3428 s (IR), 3430 w (Ra)	3595	230	68	E′
3330−3090 vbr (IR, Ra)				
3070−3020 br (IR, Ra)				
1677 m (IR), 1677 w (Ra)	1700	862	4	E′
	1671	0	10	A_1'
1606 vs, br (IR)	1624	1529	4	E′
1581 m (Ra)	1578	676	16	E′
	1547	0	3	A_1'
	1531	0	0	A_2'
1469 s (IR)	1483	366	0	E′
	1396	0	8	A_1'
1304 m (IR)	1319	7	0	E′
1259 w (IR)	1289	0	0	A_2'
1196 w (IR)	1179	1	1	E′
1154 w (IR), 1155 s (Ra)	1173	0	28	A_1'
938 w, br (IR)	1068	21	0	E′
	1058	0	0	A_2'
	1003	0	2	E′
802 s (IR)	826	58	0	A_2''
	786	0	0	E′
	776	0	0	E″
	749	2	0	A_2''
	742	0	9	A_1'
	728	0	0	E″
	654	0	0	A_2'
	601	0	4	E″
	600	0	0	A_1''
	582	0	0	E′
545 s (Ra)	531	0	49	A_1'
	449	0	7	E′
	391	0	0	A_2'
	289	3	3	E′
	255	80	0	A_2''
	249	0	0	E″
	223	0	0	A_1''
	128	491	0	A_2''
	121	0	1	E″
	111	7	0	A_2''
	93	0	0	E″

[a] vbr, very broad; br, broad; s, strong; m, middle; w, weak.

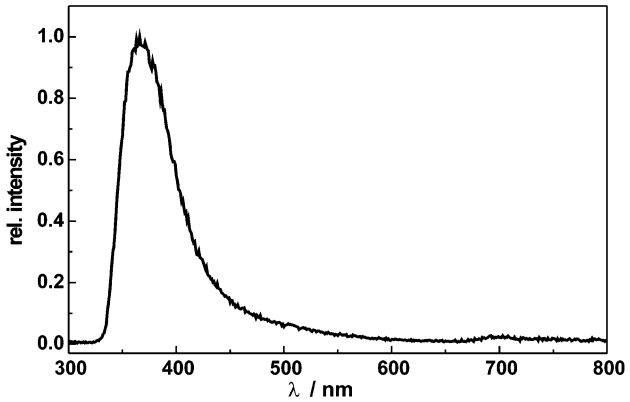

Figure 8. Photoluminescence (emission) spectrum of melem **4e**.

Thermal Behavior of Melamine. Different thermoanalytical investigations were performed to study the formation of melem during heating melamine but also to investigate the temperature stability of melem at higher temperatures.

The DSC curve of melamine shows a sharp endothermic signal at 363 °C typical for a melting process. During the cooling of the sample from 500 °C to room temperature, a sharp exothermic signal is observed at 317 °C. Therefore, the signal detected during heating is assigned to a reversible melting process which exhibits a significant hysteresis.

Temperature-dependent X-ray powder diffraction of melamine indicates several phase transitions. Between 320 and 340 °C, melamine transforms into an unknown phase. Between 360 and 380 °C, a further transition occurs which is accompanied by the formation of melem. By further heating above 520 °C, the reflections of melem disappear, and only a broad reflection at $d = 337$ pm is observed.

In further experiments, melamine was heated in sealed glass ampules to different temperatures between 380 and 500 °C. After being cooled, the reaction products remaining at the bottom of the ampules were analyzed by X-ray powder diffractometry. Apart from the reflections of the starting material melamine and the herein described melem, the reflections of at least two further intermediates were observed in the powder patterns which could not be indexed so far.

Thermal Behavior of Melem. According to temperature-dependent X-ray powder diffraction experiments between 560 and 580 °C, the reflections of melem become blurred, and above ca. 580 °C only a broad reflection at about $d = 340$ pm occurs, a value that is typical for graphite-like C−N materials.[6] Accordingly, melem is stable up to 560 °C. Above that temperature, it transforms into a C−N−H polymer without melting.

Results of the Calculations. The single free $C_6N_7(NH_2)_3$ molecule adopts D_{3h} symmetry. Optimizations with distorted initial geometry such as pyramidalized terminal amino groups or localized double bonds within the ring structure readily converged toward the high symmetrical conformation. The calculated bonds lengths and angles are given in Table 4. Apparently, the applied DFT and post-Hartree−Fock methods yield almost similar results.

To account for the possibility of different tautomeric forms of melem (as discussed in more detail within the NMR section), one proton from each amino group was shifted to a N atom of the C_6N_7 nucleus. Assuming C_{3h} symmetry, we found bond lengths for C(i)−N(c) of 129.3 and 135.4 pm and for C(e)−N(c) of 139.0 and 141.6 pm, the longer distances always to the protonated N(c) atoms. The terminal imido groups become much closer bonded; C(e)−N(t) is 127.5 pm. The data clearly indicate a strong localization of the previously delocalized bonding within the molecule. The total energy of this tautomeric form comes out 133 kJ mol^{-1} less favorable than that for D_{3h} symmetry **4e**(I). Further on, for tautomer **4e**(II) which exhibits C_s symmetry, a total energy of about 54 kJ mol^{-1} less favorable than that for D_{3h} was calculated. Hence, the calculations support the amino tautomer **4e**(I), as was independently proven by the CPPI NMR experiment discussed above.

Within the crystal structure of melem $C_6N_7(NH_2)_3$, the optimized molecular geometry came out quite similar in comparison with the free molecule in the gas phase, its local symmetry being close to D_{3h} with only minor distortions. Bond lengths and angles are given in Table 5. There is a remarkable agreement between the results for the crystal structure and those obtained for the free molecule. Noteworthy, the terminal amino groups all became almost coplanar with the C−N cyameluric nucleus of the molecule (Figure 2). Some particular effects are present, most of which are attributed to the hydrogen bonding between different molecules. The N−H bond distances are somewhat elongated within one particular amino group. The atom N(t)10 of the amino group also participates to the largest extent in the intermolecular hydrogen bonding. Moreover, while dihedral angles calculated within the C_6N_7 cyameluric nucleus do not deviate more than 2° from an ideal planar conformation, dihedrals involving hydrogen atoms indicate rotation of the almost planar terminal amino groups of up to 13°. However, the hydrogen-bond acceptors of the molecule, the N(c) atoms, appear unaffected by this kind of interaction.

The vibrational frequencies of the free $C_6N_7(NH_2)_3$ molecule were calculated using the B3LYP hybrid functional. Out of the 60 eigenmodes of the D_{3h} molecule, 7 transform as A_1', 2 as A_1'', 5 as A_2'', 6 as A_2', 14 as E′, and 6 as E″. A_2'' and E′ modes are IR-active, A_1', E′, and E″ are Raman-active, and A_1'' and A_2' are silent (inactive) modes. The eigenvalues are given in Table 6 together with the calculated relative intensities. The primed modes retain the planarity of the molecule, while double-primed modes are out-of-plane vibrations and predominantly located at lower wavenumbers. Basically, the calculated results differ by not more than 2−4% from the experimental values given in Figure 7, an agreement which is rather good and quite typical for calculations of such systems. Apparently, the six modes with the highest wavenumbers, N−H stretching vibrations above 3595 cm^{-1}, come out too high from the calculation and do not match their experimental counterparts, which are between 3000 and 3500 cm^{-1}. The reason is found in the secondary interaction of the extended hydrogen-bonding network, which causes both an elongation of N−H bonds and a slight "out-of-plane" rotation of the amino groups, leading to a decrease of the N−H stretching force constant and a significant broadening of the signals.

Summary

The occurrence of different intermediates during the condensation process of melamine according to Scheme 4 is conceivable: A condensation of two molecules of melamine under formation of the C_6N_7 ring system might be necessary.

Scheme 8. Possible Formation of Melem As Suggested by May[26]

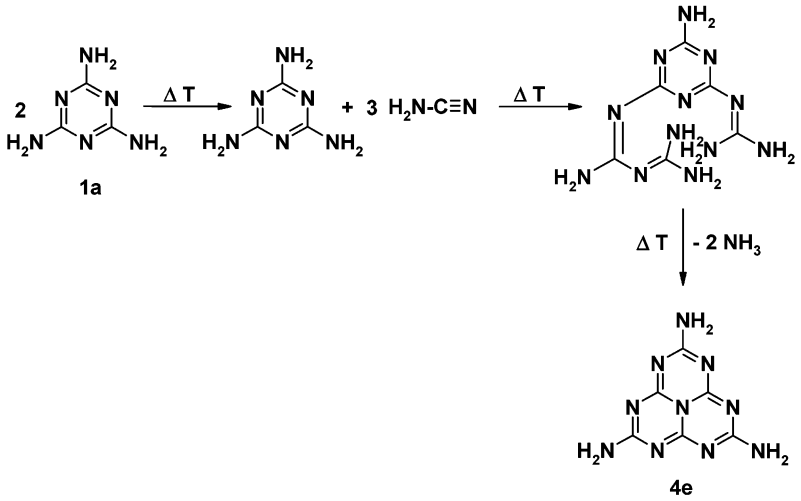

Scheme 9. Possible Formation of Melem by Reaction of Melamine **1a** with Dicyandiamide **7**

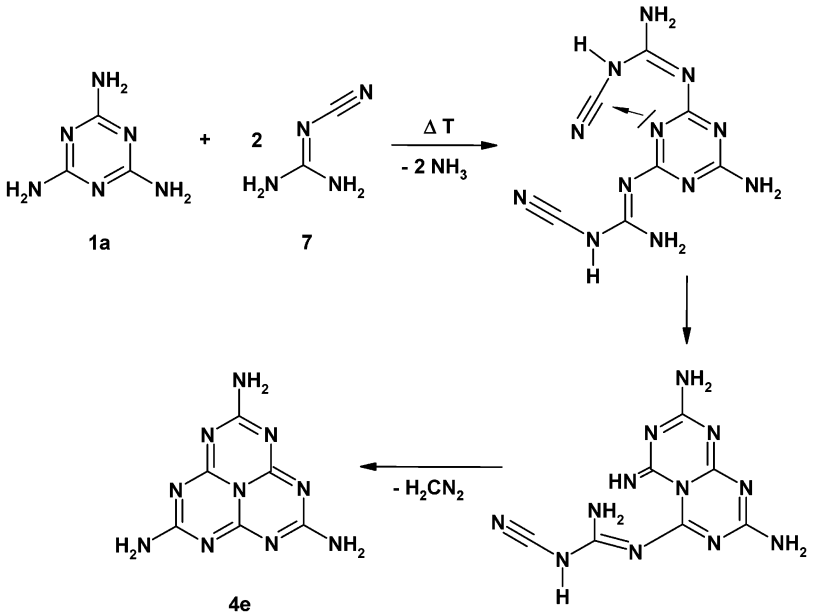

Another possible formation of melem was proposed by May:[26] During the sublimation of melamine, which starts at about 350 °C, decomposition of some melamine molecules into the monomer cyanamide H_2NCN **5** could take place. These molecules may react with nonsublimated melamine, leading to melem (Scheme 8).

Furthermore, another reaction mechanism comparable to the formation of tri-*s*-triazine described by Hosmane et al. may be possible.[20] Accordingly, the formation of melem starts from dicyandiamide: Some dicyandiamide molecules may transform into melamine which could react with nonreacted dicyandiamide molecules (Scheme 9).

Additionally, the existence of further intermediates during the condensation process is probable. For control of the condensation reaction, the specific temperature and pressure conditions during the reaction have to be adjusted carefully.

A possible way to clarify the reaction mechanism is the partial doping of the ^{15}N positions within the starting material melamine. By ^{15}N MAS NMR investigations, it might be possible to determine which types of N atoms form the ring atoms N(c) and N(i) or the amino N(t) atoms, respectively. Additionally, ^{15}N doping of the different N positions within cyanamide **5**, ammonium dicyanamide **6**, and dicyandiamide **7** should be helpful to understand the formation of melem **4e**.

In this work, we could prove the existence of melem as an important intermediate during the thermal condensation of melamine as well as of other simple C−N−H precursor compounds. The fact that melem (triamino-tri-*s*-triazine) readily forms during heating of melamine (triamino-*s*-triazine) might be indicative of a generally higher thermodynamic stability of tri-*s*-triazine derivatives and maybe even their oligomers and polymers as compared to those deriving from *s*-triazine. Therefore, it seems to be rather unlikely that within the further condensation of melem on the way to g-C_3N_4, sheets made up of *s*-triazine rings (connected by N atoms, structure **2**, Scheme 1) are formed. Therefore, we believe that graphite-like C−N materials as well as g-C_3N_4 itself formed by condensation of melamine presumably contain tri-*s*-triazine (connected by N atoms, structure **3**, Scheme 2) instead of *s*-triazine rings (structure **2**, Scheme 1). This assumption is also supported by

DFT calculations, which indicate a significantly higher stability of g-C_3N_4 based on tri-*s*-triazine building units.[17]

Acknowledgment. The authors are indebted to the following people for conducting the physical measurements: Dagmar Ewald and Dr. Gerd Fischer (mass spectrometry), Sascha Correll (temperature-dependent X-ray powder diffractometry), and Stefan Rannabauer (differential scanning calorimetry) (all Department Chemie, LMU München), as well as Dr. Thomas Jüstel and Dieter Wädow (Philips Research Laboratories Aachen) for the photoluminescence spectroscopy. Fruitful discussions with Prof. Hendrik Zipse (Department Chemie, LMU München), and especially with Prof. Edwin Kroke (Universität Konstanz), are gratefully acknowledged. Financial support by the Fonds der Chemischen Industrie, the Bundesministerium für Bildung und Forschung, and the Deutsche Forschungsgemeinschaft is also gratefully acknowledged.

Supporting Information Available: Crystallographic information (CIF). This material is available free of charge via the Internet at http://pubs.acs.org.

JA0357689